



Multiscale Interface Behaviour and Performance of GF-PC Composite

Conference Paper**Author(s):**

Vetterli, Oliver; [Pappas, Georgios A.](#) ; [Ermanni, Paolo](#) 

Publication date:

2022

Permanent link:

<https://doi.org/10.3929/ethz-b-000595509>

Rights / license:

[Creative Commons Attribution 4.0 International](#)

MULTISCALE INTERFACE BEHAVIOUR AND PERFORMANCE OF GF-PC COMPOSITE

O. Vetterli ^a, G. A. Pappas, P. Ermanni

a: Laboratory of Composite Materials and Adaptive Structures, Swiss Federal Institute of Technology Zurich (ETHZ); ^aoliverve@ethz.ch

Abstract: *Fibre-matrix interface performance is essential in fibre reinforced polymer composites, leading to important efforts in quantification and optimization. This is even more relevant for thermoplastics, since interfacial bonding happens only via physical interactions. Standardised mechanical tests provide homogenized composite properties, but fail to isolate the contribution of the interface. Micromechanical ones are designed for this exact purpose, but need complex set-ups and sample preparation. This study adopts a novel multiscale approach to measure mechanical properties of polycarbonate-glass fibre composites, manufactured under different interfacial conditions (sized & desized). This is enabled by use of focused ion beam in precise manufacturing and post-mortem analysis of specimens. The results show an evident difference between tested conditions at the macroscale (mode I), where sized specimens outperform desized ones. At the microscale (mode II), these differences are less pronounced due to the high ductility of the matrix resulting in a cohesive failure of the composite.*

Keywords: Polycarbonate; Glass fibre composites; Microscale; Interface

1. Introduction

The demand for high performing glass fibre (GF) reinforced polymer composites has been growing rapidly, mainly due to their attractive performance to price ratio, making them appealing for lightweight structures [1, 2]. Moreover, due to the sustainability potential, thermoplastic polymers are becoming a valid alternative to thermosets [3]. Also, thermoplastics like polycarbonate (PC), show very high tenacity due to their high ductility, making them appealing for demanding applications such as protective equipment and ballistics [4, 5]. Generally, the performance of composites, not only depends on the constituent material mechanical properties and orientation, but largely, on the interfacial strength [6, 7]. Interactions at this level include physical (like Van der Waals interactions), mechanical (like surface roughening) and chemical (like covalent bonds). In practical terms, bonding is improved via the application of sizing solution, which are complex mixtures that have to fulfil specific requirements [8, 9]. Contrary to thermosets, which are polymerised in-situ, thus, allowing for chemical interaction, thermoplastics only allow for physical interactions with the fibre and sizing.

Being able to precisely quantify interface strength and toughness is of paramount importance to enable the production of better performing composites, and can be done explicitly via micromechanical experiments. Unfortunately, these kind of tests are extremely laborious, lack standards and the high complexity of testing setups prevents direct comparison of results. This limits their implementation at an industrial level, where conventional macro-mechanical tests are used considering a homogenized behaviour [10]. This work will therefore focus on

investigating the failure behaviour of PC-GF composite at different size scales and processing conditions, via state of the art macromechanical test and innovative micromechanical setup. The micromechanical test set-up resembles designs applied in ceramics [11, 12] and thermosets [6, 13] composites, namely push-out test; where the interface between the matrix and fibre is forced into failure under shear (mode II). However, to precisely control the sample dimension and quality, an innovative manufacturing technique that employs a focus ion beam (FIB) has been developed. Macromechanical testing was also included in this study via transverse tensile test on laminated strip-coupons. In terms of processing conditions, a thermoplastic compatible sized glass fibre mat is compared to a neat one, where the matrix-fibre interface is expected to be lower affecting the overall performance.

2. Materials & Methods

2.1 Materials

Specimens for both macro- & micro-mechanical testing were produced with the same constituent materials. Two types of glass fibre mats were used, 92145 and 92145-FE800, produced by *Porcher Industries Germany GmbH*. Both materials are unidirectional GF mats with a nominal areal weight of $223 \pm 5 \text{ g/m}^2$ (10 g/m^2 weft direction). The only difference is the finishing of the glass fibres. The first one has been fully de-sized via thermal processing (a procedure carried out by the supplier), and the second has a thermoplastic sizing containing silane compounds. The polymeric matrix used is a commercial-grade polycarbonate *Makrofol 1-4 010181*, produced by *Covestro Germany GmbH* in film form with a thickness of 175 μm .

2.2 Macromechanical specimen manufacturing and testing set-up

Composite plates were prepared via the state-of-the-art film stacking technique, where a $200 \times 200 \text{ mm}^2$ film of polycarbonate is alternated every two layers of a $200 \times 200 \text{ mm}^2$ GF mat, for a total of 6 and 12 layers respectively. This lay-up gives a final nominal fibre volume fraction (FVF) of $\sim 54\%$ after a $\sim 2.5\%$ of matrix bleed.

The laminates were stacked manually and pressed under vacuum. To achieve flat specimens with homogeneous thickness, the material was pressed in a *Fontijne TP 400* hot press, between thick steel plates equipped with 2 mm (nominal) thick spacers to avoid excessive bleeding and restrain over-compaction. The material was heated at a constant rate of $5^\circ\text{C}/\text{min}$ up to 320°C under vacuum to avoid degradation. Once the processing temperature was reached, pressure was applied in two steps to facilitate compaction and impregnation: 10 min at 8 bar followed by 20 min at 20 bar. The whole set-up was cooled down to room temperature over a time of 40 min to relax out thermal stresses. Specimens were cut to dimension with a water-cooled circular saw according to ASTM D3039 [14] standards for transverse tensile testing. From each type of plate (2 conditions), 7 samples were produced with nominal values of length $L = 200 \text{ mm}$ width $w = 25 \text{ mm}$ and thickness $t = 2 \text{ mm}$. Prior to testing, quality control was carried out via thermogravimetric analysis (*TGA-2 SF, Mettler Toledo*) and microscopy (*VHX-6000, Keyence*) to evaluate FVF, void content and microstructure.

2.3 Micromechanical specimen preparation and testing set-up

Micromechanical specimens for the push-out geometry were made from the same laminate prepared for transverse tensile test to remove any processing bias. According to the process, initially, strip coupons with the same dimensions as the macromechanical samples are

manually ground and polished on top and side faces, via a *Tegramin-20, Streuers*, down to a surface roughness of 1 μm . The second step, consists of cutting the polished strips with a fine diamond blade (paying great care not to damage the 2 polished edges), to a final dimension of $8 \times 5 \times 2 \text{ mm}^3$ before fixing it on a scanning electron microscope (SEM) stub with conductive silver glue. Consequently, in order to successfully image the sample with an SEM, a platinum-palladium conductive coating is applied with a thickness of 10 nm via a *CCU-010 Metal Sputter Coater, Safematic* (Figure 1). In the final two steps, the sample is further smoothed and small 'pockets' are milled, by means of a focus ion beam (FIB) *Helios 5 UX Dual Beam, ThermoFisher Scientific*. The previously prepared sample is then mounted on a 45° pre-tilt adaptor and re-inserted into the device.



Figure 1: Micromechanical specimen preparation and workflow (not to scale). Left: The top ($25 \times 100 \text{ mm}^2$) and side ($25 \times 2 \text{ mm}^2$) faces are manually polished. Middle: micromechanical sample is sliced. Right: The sample is mounted on an SEM stub (not shown) and a pocket is milled via FIB.

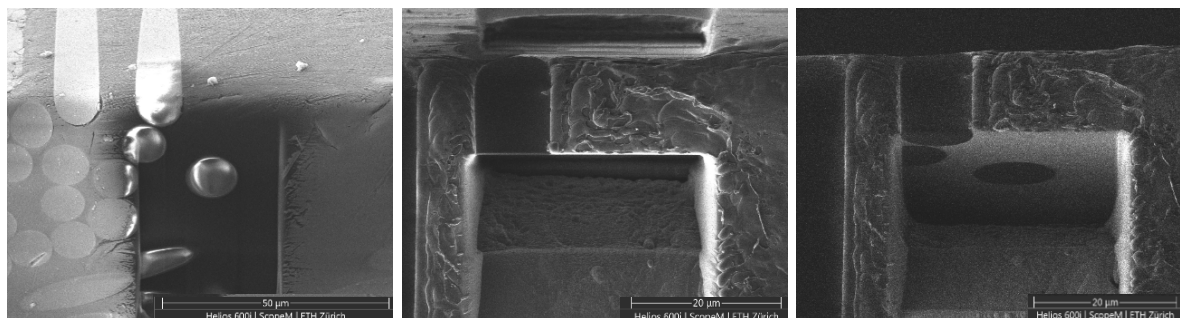


Figure 2: Detail of specimens prepared with the FIB. Left: top view of the polished surface. Middle: front view of the composite layer where the push-out test will be performed. Right: inside view of the pocket, with the single fibre domain prepared for mechanical test.

In detail, once a suitable area has been identified (matrix rich domains with isolated fibre), the top surface is further polished at a stage tilt of 8.5° (1.5° over tilt *w.r.t.* ion source), using cleaning cross sections (CCS). To achieve optimal smoothness, two procedures are run: first, a $30 \times 30 \mu\text{m}^2$ area is processed with a current of 20 nA. This removes any surface features in the micro-metre range. Secondly, a smaller area of $20 \times 20 \mu\text{m}^2$ is further processed with a finer current of 9 nA, removing sub-micrometre features.

Then the pocket, where the fibre will be pushed in, is carved out in two steps, both carried out with a gallium ion beam equipped with a water gas nozzle (multichem gun) to enhance the etching rate. First, the bulk material is removed via a regular cross-section (RCS), with a width of 3 times the fibre diameter, 30 μm depth and 20 μm height. Then a further polishing step, with a lower current of 9 nA, is carried out to achieve a smooth finishing of the newly manufactured pocket surface. Depictive SEM images are shown in Figure 2.

The previously prepared push-out samples were tested on *Vega 3 Tescan* SEM equipped with a displacement controlled indenter from *Alemnis*. For the experimental campaign, a 3.5 μm

diamond flat punch indenter, from Synton MDP, with a displacement rate of 50 nm/s was used [13].

3. Results & Discussion

The stress-strain plots in Figure 4 together with Table 1 summarize the essential information gathered from the transverse tensile tests. In both cases, sized & desized condition, five specimens provided usable results; for the rest the coupons failed close to the gripping region of the tensile machine clamp, invalidating the results [14].

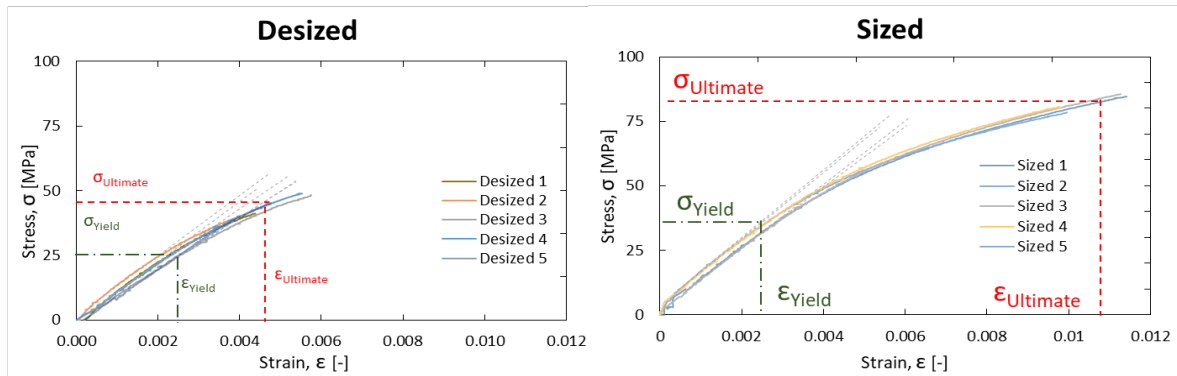


Figure 3: Tensile testing results, plot of Stress vs. Strain values of Left: Desized and Right: Sized GF-PC composite. Dotted red and green line pinpoint the measured ultimate and yield values for strength/strain, respectively.

Table 1: Macromechanical results (averages of $n=5$, and standard deviation) from transverse tensile test. *Normalized for FVF= 53.5% and pure UD assumption (without weft effect see text for details)

Material		Strength* [MPa]		Critical Strain [-]	E_{22} * [GPa]
Sized	σ_{Yield}	31.1±2.2	ϵ_{Yield}	0.0024±0.0006	12.2±0.5
	$\sigma_{Ultimate}$	78.3±3.0	$\epsilon_{Ultimate}$	0.0110±0.0005	
Desized	σ_{Yield}	24.1±3.5	ϵ_{Yield}	0.0027±0.0006	11.0±0.6
	$\sigma_{Ultimate}$	37.8±4.3	$\epsilon_{Ultimate}$	0.0051±0.0007	

Thanks to the precise manufacturing of the laminate, the void content is <0.5% and the final FVF is 53.7±0.4%; resulting in a fair and reliable comparison between the two tested conditions. To calculate the composite strength and modulus in transverse direction, the contribution of the weft (perpendicular to the bundles in the main fibre direction of the unidirectional fabric) had to be taken into account. In fact, the measured stress-strain response is assumed to be the result of pure 90° (transverse) composite plus the longitudinal glass fibre weft. One can assume the rule of mixtures (ROM, i.e. uniform strain) as a representative approximation of this combination [15]. The theoretical transverse modulus of the pure GF-PC composite in the transverse direction can be approximated by the Halpin-Tsai semi-empirical model (Eq. 1, with $\xi = 2$), which in combination with the weft contribution provides a value for the given ratio of weft and UD. This is then compared with the effective measured modulus, providing a correction factor, in the range of 0.8, for the measured stresses, allowing the evaluation of the true strength in the transverse direction. Moreover, to be consistent with the micromechanical evaluation of the material, yield strength was defined by a 2% deviation from linearity [13].

$$E_{22} = E_{PC} \frac{1 + \xi \eta \nu_f}{1 - \eta \nu_f}, \text{ with } \eta = \frac{E_{GF} - E_{PC}}{E_{GF} + \xi E_{PC}} \quad (1a)$$

$$E_{22}^* = \frac{\nu_f}{\nu_f + \nu_w} E_{22} + \frac{\nu_w}{\nu_f + \nu_w} E_{GF} \quad (1b)$$

In Eq. 1a & 1b, E_{22} is the modulus in transverse direction; ν_f is the fibre volume fraction in the principal direction; ν_w is the weft-fibre volume fraction; E_{GF} , E_{PC} the moduli of glass fibre and matrix respectively; Note that the total FVF= $\nu_f + \nu_w$.

From the provided data, a substantial influence of sizing can be observed. Compared to desized samples, sized conditions have 52% and 23% higher ultimate and yield strength, respectively. Ultimate strain results follow the same trend, too, with sized conditions having a 54% higher value compared to desized. Though, yield strain values are in the same order of magnitude for both tested conditions. E-moduli have a more contained difference (10%); nonetheless, the overall trend is repeated in this instance too.

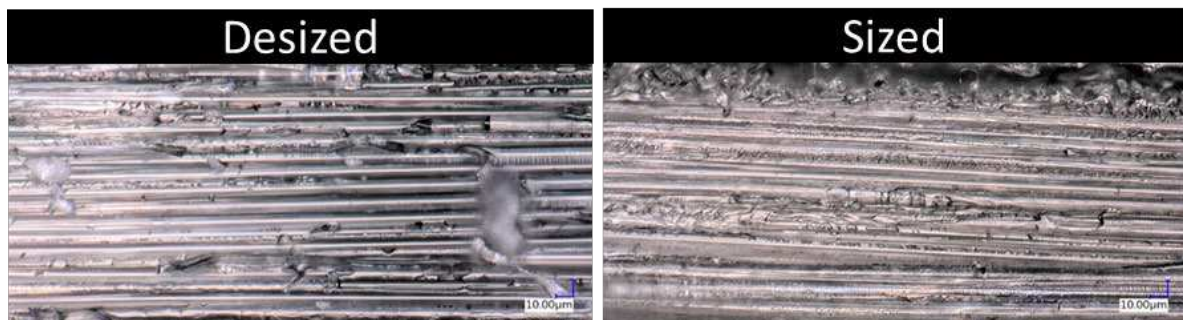


Figure 4: Fractography on surfaces resulting from tensile test. *Left: desized surface, with mainly adhesive failure as a result of a weaker matrix-fibre interface. Right: sized surface, with mixed adhesive-cohesive failure.*

Interestingly, the presence of sizing allows for a much larger plastic deformation before failure. This can be explained by a stronger interface between the two components and can be seen in the post-mortem microscopy analysis of the cracked specimens, similar to the observations of Montenegro et. al. [16] (Figure 5). Sizing leads to a failure with partially coated fibres after the tensile test, leading to a mixed adhesive-cohesive failure. For desized condition, a considerably larger bare glass fibre surface is exposed, resulting in a predominantly adhesive failure of the specimen. This behaviour observed at the macro scale can be partially seen at the micro-scale too, where the bottom portion of the pushed-out fibre is partially matrix coated for the sized sample and bare for the desized one (Figure 6) as explained hereafter.

In Figure 7 the results from the push-out tests are reported. The nominal effective shear stress is calculated over the contact area between the glass and matrix, where $F_{applied}$ is the force applied by the indenter, r the fibre radius and h the height of the composite layer (Eq. 2). Via this simple calculation, differences in fibre diameter and polymer layer thickness can be accounted for. The first portion of the curve with the initial rise and constant slope, was a result of elastic bending of the thin composite layer and elastic response of the fibre. This was followed by a flattening of the curve and the approaching of critical load where failure happened. Though, in our case, since the interface was stronger than the polymer, contrary to ceramic and often thermoset matrices, this portion of the graph corresponded, mainly, to the plastic deformation of the polymer. Nonetheless, a critical load (marked with a star) has been identified at 2% deviation from linearity, following previously reported procedure on similar geometry [6, 17].

$$\tau_{Nominal} = \frac{F_{applied}}{2 \pi r h} \quad (2)$$

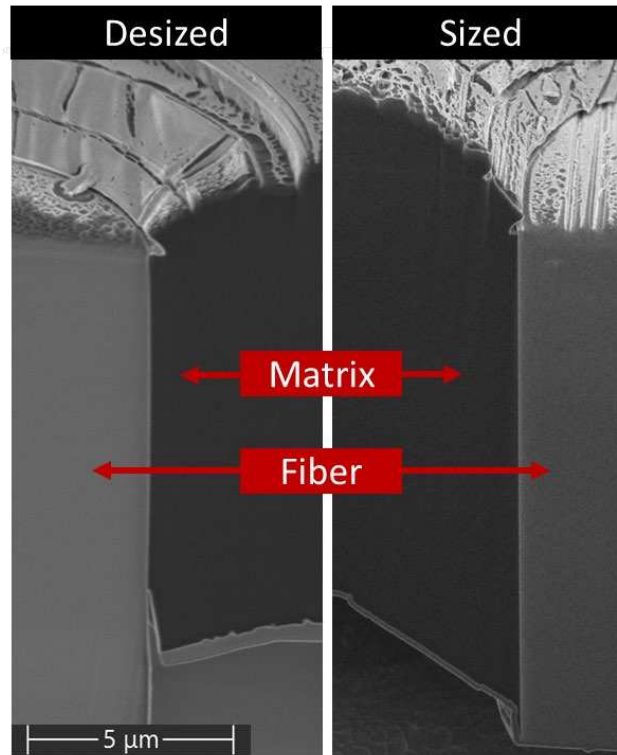


Figure 5: SEM picture of the cross-section of a pushed out fibre.. *Left*: Desized fibre, where it can be seen that the interface at the bottom of the specimens fails adhesively. *Right*: Sized fibre, where it can be seen that the matrix has been plastified extensively, and the pushed-out portion of the fibre still has matrix on the surface, leading to a cohesive failure. Note that, the final displacement and force applied is higher for the sized one.

The average value for critical shear stress for sized and desized conditions are 31.0 ± 0.9 MPa and 27.1 ± 2.5 MPa respectively. These values do not correspond to a complete interface failure, because the polymer yields extensively without any pronounced interface failure (Figure 6). This phenomenon is attributed to an interface strength in mode II higher than the matrix shear strength, compared to mode I vs. tensile strength (as in the case of transverse tensile test). Nonetheless, the overall trends can be retrieved and give useful insights into the failure mechanisms.

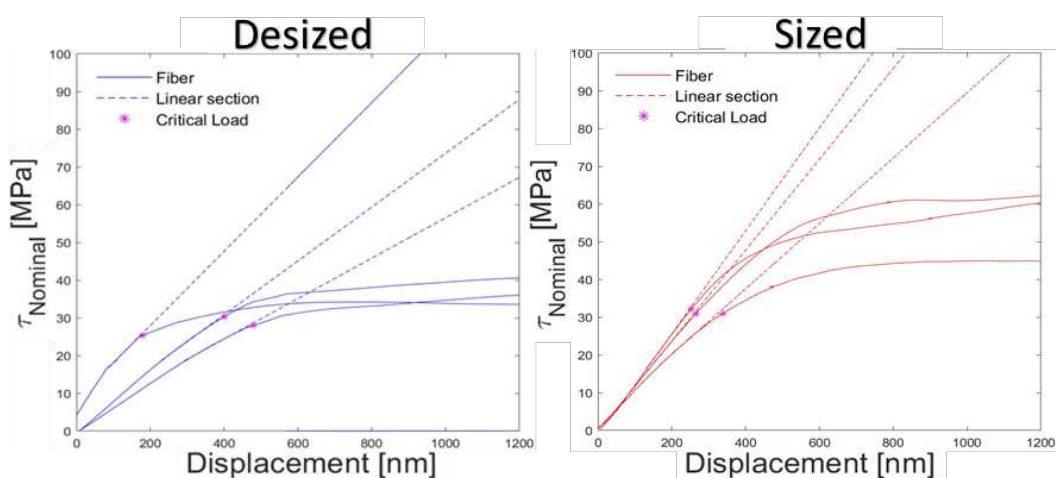


Figure 6: Results of Nominal shear (Eq. 2) vs. displacement from push-out experiments on PC-GF composite (for each condition, $n=3$). *Left*: Desized and *Right*: Sized.

Once the mechanical test has been carried out, the specimen is treated, once more, with the FIB to obtain the post-mortem samples (Figure 6). The pushed-out fibre is cut in fibre direction to better visualise the interface between the components and plastic deformation of the matrix. When inspecting this newly manufactured cross-section, a substantial difference can be observed at the bottom end of the layer. This domain is loaded under shear but also tensile stress (due to bending), i.e. partially mixed-mode conditions. Therefore, the interface fails cohesively for the sized sample and partially adhesively for the desized one, following similar trends as in the macromechanical tests. This can be recognised by the fully exposed glass fibre surface for the desized condition (bottom portion of Figure 6, left). On the other hand, in the small portion that has been pushed out in the sized condition, the fibre surface retain a thin layer of polymer (bottom portion of the figure, right), and extensive yielding of the polymer can be observed. Thus, composite action was maintained for a large portion of the experiment in both cases, with essentially cohesive failure, yet, showing a stronger interface than in the desized condition.

4. Conclusion & Outlook

Mechanical analysis of PC-GF composites at different size scales allowed us to identify, quantify and visualise the failure behaviour of this understudied thermoplastic fibre reinforced material. By implementing a FIB procedure in the manufacturing and analysis of the samples, a reliable and precise micromechanical, interface-evaluation scheme has been implemented for thermoplastic composites. In terms of mechanical properties, as expected, the material with the thermoplastic compatible sizing applied to the surface of the glass fibre, performs better at both size scales than the desized one. Moreover, the failure mechanism under transverse tensile loading can be clearly identified by the post mechanical test analysis, where the failure is predominately adhesive and mixed adhesive-cohesive, for desized and sized conditions, respectively.

Thanks to the use of FIB, which allows us to process the specimen after micromechanical testing, the main tendencies observed at the macro scale can be identified at the single fibre level too, contributing to the multi-scale mechanical analysis.

Due to the high degree of ductility of the thermoplastic polymer, as well as the high strength of the PC-GF interface under mode II, the fibre cannot be fully separated (pushed-out) from the matrix. This behaviour diverges from the commonly observed one for thermosets and ceramics. In detail, a brittle interface will lead to a complete separation, but also brittle matrix cracking will have similar effect with a wet fibre though (cohesive failure).

Thus, for PC-GF combination, where we observe high ductility and good interface in mode II, novel micromechanical tests shall be developed and further optimised to achieve a complete interface failure and strength identification. This could be achieved via finite element analysis, where the mechanical contribution of neighbouring fibres, shear and bending forces on the specimen geometry could be simulated to provide insights into mode II interface failure. Of great interest would be to develop a micromechanical test able to induce interface failure in mode I. This would be beneficial since it would allow a more representative comparison to the macromechanical test. Even though, the latter has great complexity, it will allow gaining a better understanding of failure mechanisms at a microscopic level.

Acknowledgments

The authors thank Reuteler Joakim of ScopeM-ETH Zurich and Lauener Carmen from the Laboratory of Nanometallurgy ETH Zurich for their support & assistance in this work.

Reference

- [1] C. Schneeberger, N. Aegerter, S. Birk, S. Arreguin, J. Wong und P. Ermanni, «Direct stamp forming of flexible hybrid fibre preforms for thermoplastic composites,» in *SAMPE Europe Conference 2020 Amsterdam: The Future Composite Footprints*, 2021.
- [2] C. Schneeberger, J. C. H. Wong und P. Ermanni, «Hybrid bicomponent fibres for thermoplastic composite preforms Part A Applied science and manufacturing,» 2017.
- [3] J. L. Thomason, «Glass fibre sizing: A review,» *Composites Part A: Applied Science and Manufacturing*, Bd. 127, p. 105619, 2019.
- [4] S. Fu, Y. Wang und Y. Wang, «Tension testing of polycarbonate at high strain rates,» *Polymer Testing*, Bd. 28, p. 724–729, 2009.
- [5] N. A. Fleck, W. J. Stronge und J. H. Liu, «High strain-rate shear response of polycarbonate and polymethyl methacrylate,» *Proceedings of the Royal Society of London. A. Mathematical and Physical Sciences*, Bd. 429, p. 459–479, 1990.
- [6] C. Medina M, J. M. Molina-Aldareguía, C. González, M. F. Melendrez, P. Flores und J. LLorca, «Comparison of push-in and push-out tests for measuring interfacial shear strength in nano-reinforced composite materials,» *Journal of Composite Materials*, Bd. 50, p. 1651–1659, 2016.
- [7] C. González und J. LLorca, «Mechanical behavior of unidirectional fiber-reinforced polymers under transverse compression: microscopic mechanisms and modeling,» *Composites Science and Technology*, Bd. 67, p. 2795–2806, 2007.
- [8] J. L. Thomason, «Interfacial strength in fibre reinforced thermoplastics,» in *International Conference on Interfaces & Interphases in Multicomponent Materials (IIMM)*, 2010.
- [9] J. Karger-Kocsis, H. Mahmood und A. Pegoretti, «Recent advances in fiber/matrix interphase engineering for polymer composites,» *Progress in Materials Science*, Bd. 73, p. 1–43, 2015.
- [10] F. R. Jones, «A review of interphase formation and design in fibre-reinforced composites,» *Journal of Adhesion Science and Technology*, Bd. 24, p. 171–202, 2010.
- [11] R. M. G. De Meyere, K. Song, L. Gale, S. Harris, I. M. Edmonds, T. J. Marrow, E. Saiz, F. Giuliani, D. E. J. Armstrong und O. Gavaldà-Díaz, «A novel trench fibre push-out method to evaluate interfacial failure in long fibre composites,» *Journal of Materials Research*, Bd. 36, p. 2305–2314, 2021.
- [12] R. S. Hay, E. E. Boakye, P. Mogilevsky, G. E. Fair, T. A. Parthasarathy und J. E. Davis, «Transformation Plasticity in (Gd x Dy 1- x) PO 4 Fiber Coatings During Fiber Push Out,» *Journal of the American Ceramic Society*, Bd. 96, p. 1586–1595, 2013.
- [13] F. Naya, J. M. Molina-Aldareguia, C. S. Lopes, C. González, LLorca und J, «Interface characterization in fiber-reinforced polymer–matrix composites,» *Jom*, Bd. 69, p. 13–21, 2017.

- [14] A. C. D.-3. on Composite Materials, Standard test method for tensile properties of polymer matrix composite materials, ASTM international, 2008.
- [15] I. M. Daniel, O. Ishai, I. M. Daniel und I. Daniel, Engineering mechanics of composite materials, Bd. 1994, Oxford university press New York, 2006.
- [16] D. M. Montenegro, G. Pappas, J. Botsis, M. Zogg und K. Wegener, «A comparative study of mode I delamination behavior of unidirectional glass fiber-reinforced polymers with epoxy and polyurethane matrices using two methods,» *Engineering Fracture Mechanics*, Bd. 206, p. 485–500, 2019.
- [17] H. Ho und L. T. Drzal, «Evaluation of interfacial mechanical properties of fiber reinforced composites using the microindentation method,» *Composites Part A: Applied Science and Manufacturing*, Bd. 27, p. 961–971, 1996.